

**Second-line rituximab, lenalidomide, and bendamustine in mantle cell lymphoma: a phase II clinical trial of the Fondazione Italiana Linfomi**

Shunsuke Hatta,<sup>1,2</sup> Tohru Fujiwara,<sup>1</sup> Takako Yamamoto,<sup>2</sup> Kei Saito,<sup>1</sup> Mayumi Kamata,<sup>1</sup> Yoshiko Tamai,<sup>3</sup> Shin Kawamata<sup>2</sup> and Hideo Harigae<sup>1</sup>

<sup>1</sup>Department of Hematology and Rheumatology, Tohoku University Graduate School of Medicine, Sendai; <sup>2</sup>Division of Cell Therapy, Foundation of Biomedical Research and Innovation, Kobe and <sup>3</sup>Department of Gastroenterology and Hematology, Hirosaki University Graduate School of Medicine, Japan

Correspondence: harigae@med.tohoku.ac.jp  
doi:10.3324/haematol.2017.179770

## Supplementary Figure legends

### Supplementary Figure 1. A case of XLSA

(A) Representative picture of ring sideroblasts (Prussian blue stain). (B) The *ALAS2* mutation, showing a T to C substitution (c.1737) was detected using genomic DNA from whole blood.

### Supplementary Figure 2. Generation and phenotyping of patient-derived bone marrow mesenchymal stem cells (BM-MSCs)

(A) Morphology of BM-MSCs derived from a patient with X-linked sideroblastic anemia (XLSA). Scale bar, 200  $\mu$ m. (B) Differentiation of BM-MSCs. The osteogenic cell layer exhibited positive alkaline phosphatase staining. Typical adipocytes contained oil drops that stained positively with Oil Red O. (C) Human BM-MSCs expressed cell-surface antigens characteristic of BM-MSCs. The analysis confirmed that the BM-MSCs expressed typical markers (e.g., CD29, CD44, CD90, and CD105) but not CD14, CD34, or CD45. (D) Sanger sequencing of XLSA-derived BM-MSCs showing a T to C substitution (c.1737) in the *ALAS2* gene.

### Supplementary Figure 3. Generation and characterization of X-linked sideroblastic anemia (XLSA)-derived induced pluripotent stem (iPS) cells

(A) The experimental scheme for generating iPS cells from bone marrow mesenchymal stem cells (BM-MSCs). (B) Immunofluorescence staining of spontaneously differentiated NiPS and XiPS cells from embryoid bodies. Scale bar, = 50  $\mu$ m.

**Supplementary Figure 4. Evaluation of pluripotency for established iPS cells**

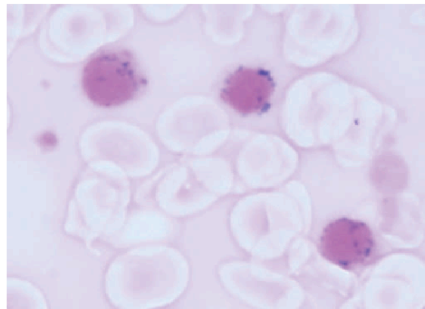
(A) Immunofluorescence staining of embryoid bodies-based spontaneously differentiated XiPS and NiPS. Immunohistochemical staining against AFP (endoderm),  $\alpha$ -SMA (mesoderm), and  $\beta$ -tubulin (ectoderm) were shown. Scale bar, 50  $\mu$ m. (B) Hematoxylin and eosin staining of teratomas obtained via subcutaneous injection of XiPS and NiPS cells. Histological examination confirmed that these tumors were teratomas containing tissues from all three germ layers, including neural epithelium (ectoderm), cartilage (mesoderm), and gut-like epithelium (endoderm). Ectoderm scale bar = 50  $\mu$ m. Mesoderm and endoderm scale bars = 200  $\mu$ m.

**Supplementary Figure 5. Morphological analysis of NiPS- and XiPS-derived erythroblasts**

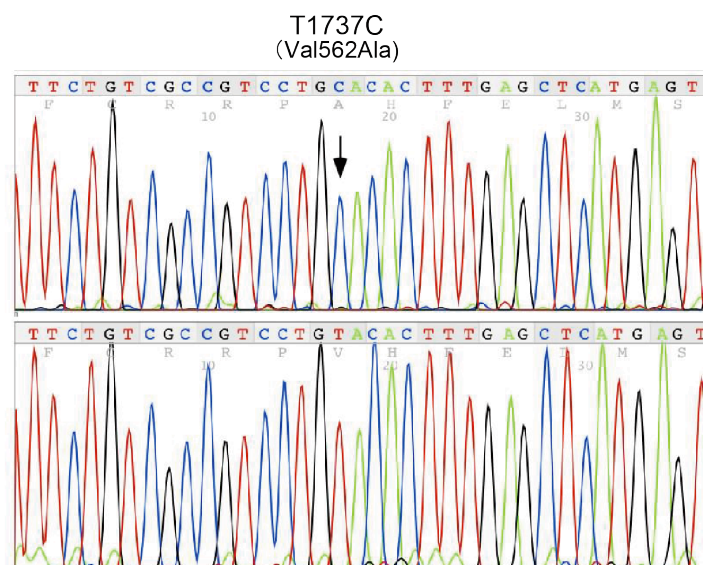
May–Giemsa staining of NiPS- and XiPS-derived erythroblasts were shown.

Supplementary Figure 1

A

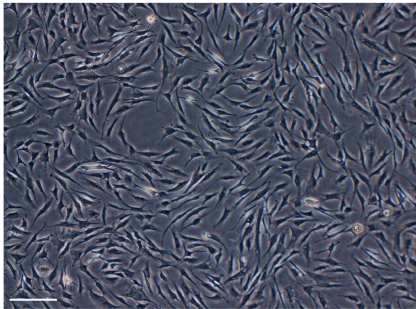


B

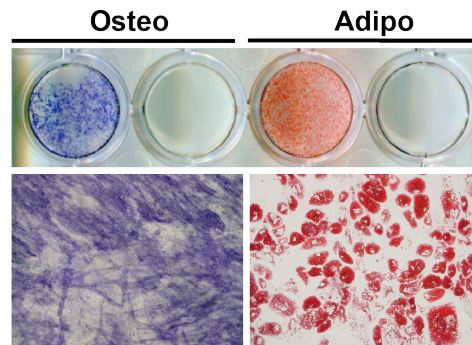


Supplementary Figure 2

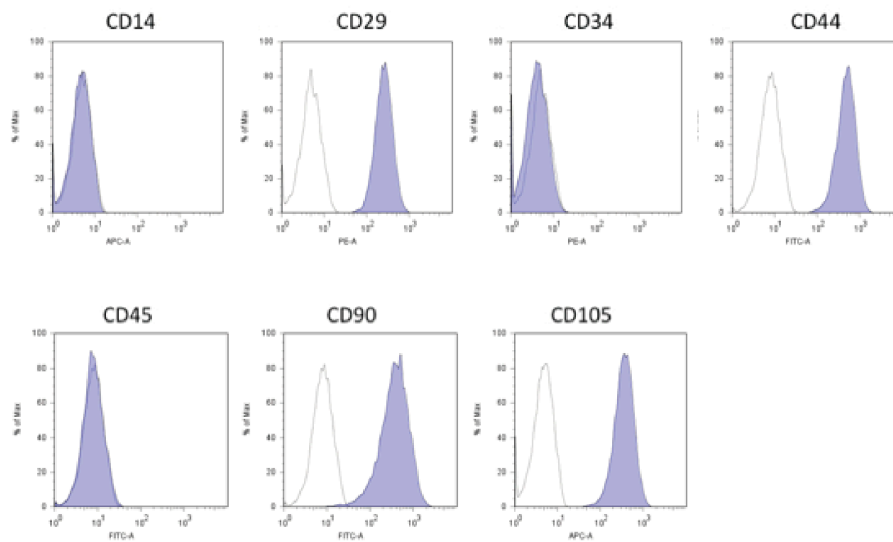
A



B

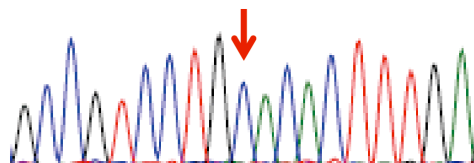


B

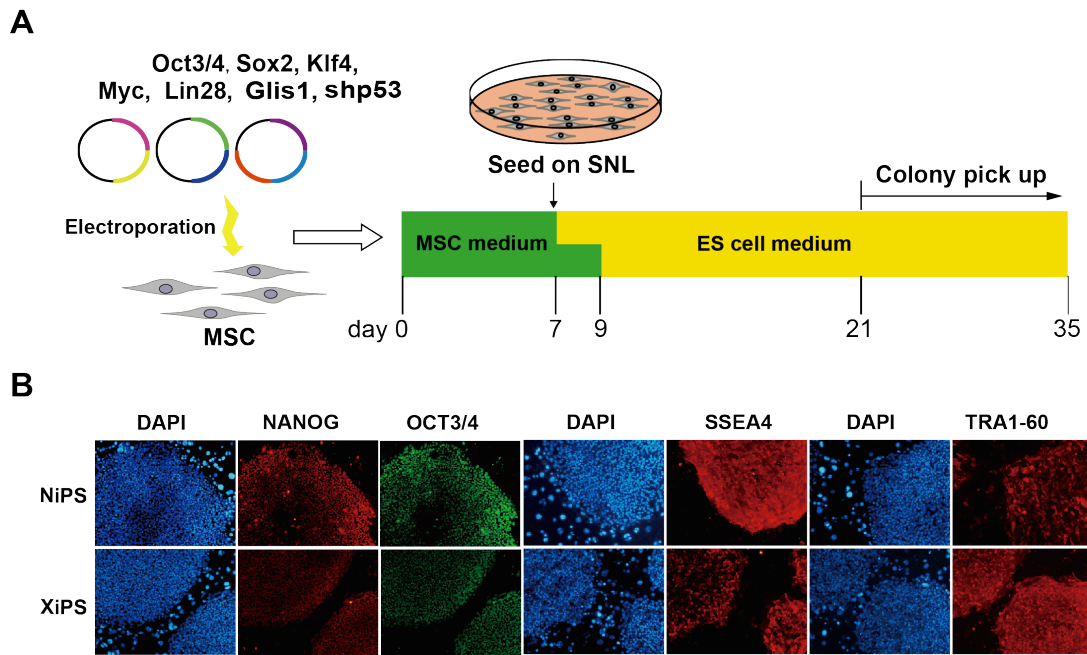


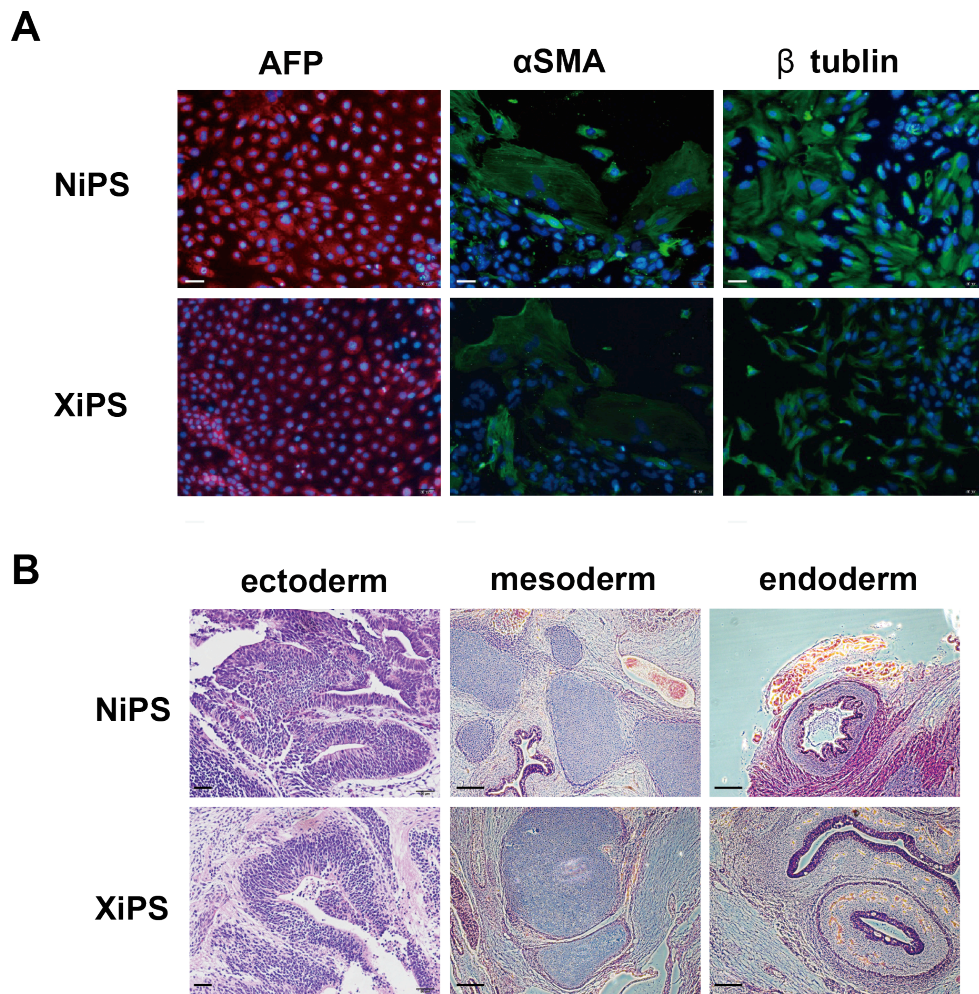
D

GCCGTCCTGCACACTTTGA



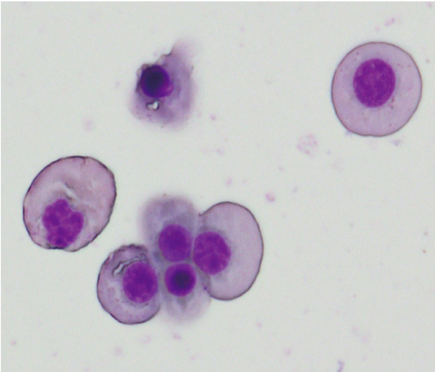
T1737C  
(Val562Ala)





Nay Giemsa Stain

NiPS-derived erythroblasts



XiPS-derived erythroblasts

